

# Generic Contrast Agents

Our portfolio is growing to serve you better. Now you have a choice.



[VIEW CATALOG](#)

# AJNR

## **Impact of Methodologic Choice for Automatic Detection of Different Aspects of Brain Atrophy by Using Temporal Lobe Epilepsy as a Model**

C. Scanlon, S.G. Mueller, D. Tosun, I. Cheong, P. Garcia, J. Barakos, M.W. Weiner and K.D. Laxer

This information is current as of May 28, 2025.

*AJNR Am J Neuroradiol* 2011, 32 (9) 1669-1676

doi: <https://doi.org/10.3174/ajnr.A2578>

<http://www.ajnr.org/content/32/9/1669>

ORIGINAL  
RESEARCH

C. Scanlon  
S.G. Mueller  
D. Tosun  
I. Cheong  
P. Garcia  
J. Barakos  
M.W. Weiner  
K.D. Laxer



# Impact of Methodologic Choice for Automatic Detection of Different Aspects of Brain Atrophy by Using Temporal Lobe Epilepsy as a Model

**BACKGROUND AND PURPOSE:** VBM, DBM, and cortical thickness measurement techniques are commonly used automated methods to detect structural brain changes based on MR imaging. The goal of this study was to demonstrate the pathology detected by the 3 methods and to provide guidance as to which method to choose for specific research questions. This goal was accomplished by 1) identifying structural abnormalities associated with TLE with (TLE-mts) and without (TLE-no) hippocampal sclerosis, which are known to be associated with different types of brain atrophy, by using these 3 methods; and 2) determining the aspect of the disease pathology identified by each method.

**MATERIALS AND METHODS:** T1-weighted MR images were acquired for 15 TLE-mts patients, 14 TLE-no patients, and 33 controls on a high-field 4T scanner. Optimized VBM was carried out by using SPM software, DBM was performed by using a fluid-flow registration algorithm, and cortical thickness was analyzed by using FS-CT.

**RESULTS:** In TLE-mts, the most pronounced volume losses were identified in the ipsilateral hippocampus and mesial temporal region, bilateral thalamus, and cerebellum, by using SPM-VBM and DBM. In TLE-no, the most widespread changes were cortical and identified by using FS-CT, affecting the bilateral temporal lobes, insula, and frontal and occipital lobes. DBM revealed 2 clusters of reduced volume complementing FS-CT analysis. SPM-VBM did not show any significant volume losses in TLE-no.

**CONCLUSIONS:** These results demonstrate that the 3 methods detect different aspects of brain atrophy and that the choice of the method should be guided by the suspected pathology of the disease.

**ABBREVIATIONS:** DBM = deformation-based morphometry; EMS = expectation maximization segmentation; FDR = false discovery rate; FS = Freesurfer; FS-CT = FS-based cortical thickness; FSL = FMRIB Software Library; FWHM = full width at half maximum; GM = gray matter; ICV = intracranial volume; SPM = statistical parametric mapping; TLE = temporal lobe epilepsy; TLE-mts = TLE-mesial temporal sclerosis; TLE-no = TLE-normal-appearing hippocampus; ULD = unbiased large deformation; VBM = voxel-based morphometry; WM = white matter

The most commonly used methods for automated whole brain structural analysis are VBM,<sup>1,2</sup> DBM,<sup>3,4</sup> and cortical thickness methods.<sup>5,6</sup> VBM is the most widely used method to date, with more than 22 studies published in the area of TLE alone.<sup>7-11</sup> One of the main reasons for its popularity is probably that VBM is relatively easy to perform, with freely available software such as SPM (Wellcome Department of Cognitive Neurology, London, United Kingdom) and FSL (FMRIB Analysis Group, Oxford, United Kingdom). The first step of so-called optimized VBM<sup>12</sup> is to generate a probabilistic GM map from the T1 gray-scale images by using a combination of voxel intensity and an a priori knowledge of the

spatial distribution of GM. GM maps are then registered to a reference image. Registration to the reference image is based on a low-dimensional spatial transformation that aligns global differences but preserves local differences in GM distribution. GM volume differences between groups are then assessed voxel by voxel by using a general linear model.

DBM differs from VBM in 2 main aspects. First, the DBM image is not segmented, so the information from the full gray-scale brain is used in the analysis. Second, DBM registration is high-dimensional, eliminating individual subject physiologic and pathologic morphology differences. The anatomic differences then lie in the deformation fields that are required to transform the subject's brain. The more precise the registration, the more sensitive the method will be to detect subtle systematic structural differences that may not be possible with VBM.<sup>13,14</sup> The downside of this technique, however, is that DBM registration algorithms are not widely available and are not as simple to implement as VBM. This is probably one of the main reasons VBM is generally used over DBM. To our knowledge, there are no whole brain DBM studies reported in TLE.

Cortical thickness is commonly computed by analyzing the 3D reconstruction of the brain's cortical surface from structural MR imaging. The freely available FS software (Martinis

Received November 1, 2010; accepted after revisions January 25, 2011.

From the Center for Imaging of Neurodegenerative Diseases and Department of Radiology (C.S., S.G.M., D.T., I.C., M.W.W.), Department of Neurology (P.G.), University of California—San Francisco and Pacific Epilepsy Program, California Pacific Medical Center (J.B., K.D.L.), San Francisco, California.

This work was supported by the National Institutes of Health grant R01NS0311966 to K.D.L.

Please address correspondence to Kenneth D. Laxer, MD, Pacific Epilepsy Program, California Pacific Medical Center, 2100 Webster St, Suite 115, San Francisco, CA 94115; e-mail: laxerkd@sutterhealth.org



Indicates open access to non-subscribers at [www.ajnr.org](http://www.ajnr.org)

<http://dx.doi.org/10.3174/ajnr.A2578>

Center for Biomedical Imaging, Massachusetts General Hospital, Boston, Massachusetts) is the most commonly used software for that purpose. FS-CT is determined as the distance from the GM/WM surface to the GM/CSF surface. The intersubject registration procedure is then based on alignment of the cortical folding patterns as opposed to the voxel intensities used for VBM and DBM. Although fluid warped images by using the DBM approach also can very precisely match the reference image, matching intensities may be less anatomically meaningful than matching cortical folding patterns. This may lead to a failure to align matching cortical regions across subjects, resulting in a lack of power in localizing subtle cortical differences in the voxel-based approaches.<sup>13</sup> The drawback of cortical thickness analysis is that it will not detect subcortical abnormalities.

The overall aim of this study was to compare VBM, DBM, and FS-CT regarding their ability to detect different types of atrophy (subtle or microscopic atrophy versus mass or macroscopic atrophy). TLE is associated with both types of atrophy and thus was chosen as a model to investigate this question. Based on the appearance of the hippocampus, TLE can be divided into 2 subgroups: TLE with MR imaging signs (hippocampal atrophy and increased T2 signal intensity) of mesial temporal sclerosis (TLE-mts) and TLE with normal MR imaging, characterized by a normal-appearing hippocampus (TLE-no). In addition to the hippocampal volume loss, TLE-mts is characterized by ipsilateral mesial and lateral temporal, but also frontal, parietal, occipital, and cerebellar volume loss as well as smaller subcortical structures (basal ganglia and thalamus).<sup>9,15,16</sup> Structural changes in TLE-no by using both VBM and region of interest approaches however are more subtle and less consistent.<sup>17-19,11</sup> Cortical thickness measurements, on the other hand, have shown widespread temporal and extratemporal cortical thinning.<sup>16</sup> Due to differences in study design, eg, measurement parameter investigated, study population, field strength, and applied statistical analysis, it is not possible to draw conclusions regarding the sensitivity of the methods used to detect these abnormalities across studies.

The aim of this study was to compare the type of volume loss detected by each method—SPM-VBM, DBM, and FS-CT—and so to provide guidance on which method may be best to adopt in answering specific research questions. We expected that in TLE-mts, where macroscopic volume abnormalities occur, all 3 methods would be sensitive enough to detect these large-scale volume changes (CT on the cortex only). However, it was expected that in TLE-no DBM would be able to detect subtle subcortical changes over VBM due to its superior coregistration. We also hypothesized that FS-CT would detect subtle cortical abnormalities, without macroscopic volume losses, not detected by either voxel-based method.

## Materials and Methods

### Subjects

Participants in this investigation consisted of 15 patients with unilateral TLE-mts (6 men, 9 women; mean age,  $40.1 \pm 9.6$  years), 14 patients with unilateral TLE-no (6 men, 8 women; mean age,  $39.6 \pm 8.3$  years), and 24 healthy controls (12 men, 12 women; mean age,  $37.9 \pm 9.4$  years). All patients were recruited during presurgical eval-

uation from the University of California, San Francisco and the Pacific Epilepsy Program, California Pacific Medical Center. A cortical thickness analysis including some of these subjects has previously been published from our laboratory.<sup>16</sup> Laterality of seizure onset was made from prolonged ictal and interictal scalp video-electroencephalogram telemetry. Nine TLE-mts patients had a left temporal onset, and 6 TLE-mts patients had a right onset. In TLE-no, 7 patients were diagnosed with left temporal onset, and 7 patients had a right temporal onset. Patients were categorized as TLE-mts or TLE-no based on evidence of hippocampal atrophy and signal intensity changes on their 4T MR imaging that used an epilepsy-specific protocol, and all were reviewed by the same neuroradiologist (J.B.). Hippocampal volumetry was used to confirm the presence (TLE-mts) or absence (TLE-no) of significant hippocampal volume loss. Volumetry was performed on high-resolution T2-weighted hippocampal images by using a method of manual segmentation.<sup>20</sup> There was a significant mean difference ( $P < .001$ ) between the age at which TLE-mts and TLE-no patients developed epilepsy (TLE-mts,  $5 \pm 6.6$  years; TLE-no,  $23 \pm 11.7$  years) and also the duration of years patients have had epilepsy (TLE-mts,  $34.6 \pm 11.8$  years; TLE-no,  $17.1 \pm 9.8$  years).

### Data Processing

**MR Imaging Acquisition.** All subjects underwent MR imaging with an MedSpec 4T system (Bruker MedSpec, Madison, Wisconsin) controlled by a Trio console (Siemens, Erlangen, Germany) and equipped with an 8-channel array coil (USA Instruments, Aurora, Ohio). A volumetric T1-weighted magnetization-prepared rapid acquisition of gradient echo sequence was acquired with the following imaging parameters: 2300/3/950 ms (TR/TE/TI); flip angle of  $7^\circ$ ; and  $1 \times 1 \times 1$ -mm<sup>3</sup> voxel resolution.

### Image Processing

To combine left and right temporal onset patients in the analysis, MR imaging data for patients were reassembled according to brain hemisphere of seizure onset. Therefore, images of the subjects with right TLE onset were left-right flipped so that all subject ipsilateral hemispheres were on the left side. Because previous studies have revealed GM asymmetries between the left and right hemispheres in the normal population,<sup>21</sup> customized symmetrical templates were generated for each analysis method from the same control subjects as described below.

### Voxel-based Morphometry

T1 images were intensity inhomogeneity corrected and segmented into GM, WM, and CSF by using the EMS toolbox<sup>22</sup> in SPM2 (<http://www.fil.ion.ucl.ac.uk/spm>), running in Matlab 6.1 (MathWorks, Natick, Massachusetts). The EMS toolbox was used as opposed to standard SPM2 due to its superior bias field correction algorithm that performs better with the more pronounced bias field of the 4T images. Optimized VBM was then carried out on probabilistic GM maps according to the optimized VBM protocol described in detail previously.<sup>12</sup> To summarize, a study-specific symmetrical SPM GM template was first created by averaging 31 normalized (first affine followed by a nonlinear registration) control subjects (flipped and unflipped) and smoothing by using an isotropic 8-mm FWHM Gaussian kernel. All GM maps were then normalized to this symmetrical template first by using a 12-parameter affine transformation, followed by a nonlinear transformation to minimize the residual squared difference between the image and template.<sup>23</sup> Voxel intensity values were multiplied (modulated) by the Jacobian determinant (ie,

the local expansion/contraction factor) derived from the deformation map produced during spatial normalization, to preserve GM volume. The modulated GM images were smoothed with an isotropic 8-mm FWHM Gaussian kernel and used for statistical analysis.

### **Deformation-based Morphometry**

The T1 images were skull-stripped, and intensity inhomogeneity was corrected by using the bias field generated by EMS. A study-specific symmetrical ULD template was created using the same 31 control subjects as for the VBM template by using a fluid registration algorithm.<sup>24</sup> This template creation step is described in full elsewhere.<sup>25</sup> To summarize briefly, it incorporates an unbiased approach in which each subject's flipped and nonflipped images are first simultaneously deformed to create a symmetrical subject brain. Symmetrical subject images are then simultaneously deformed iteratively into an average ULD template brain. This technique avoids the bias toward a particular subject's geometry introduced by selecting a single subject template.<sup>26</sup> The ULD template also contains sharper features than the multisubject average intensity template as created in SPM.

Each subject's T1 image is first registered to the template with an affine 12-parameter transformation. Subject brains are then nonlinearly deformed to the template by using a fluid-flow warping technique.<sup>25</sup> The Jacobian determinants of the deformation fields are used to gauge the local volume differences at each voxel between the individual image and the template. Each subject Jacobian map is smoothed with an isotropic 8-mm FWHM Gaussian kernel.

### **Cortical Thickness**

Analysis of cortical thickness was carried out by using FS, version 3.05 (<https://surfer.nmr.mgh.harvard.edu>). Detailed descriptions of this method have already been published<sup>27,28</sup> but are briefly summarized here. Based on a linear combination of voxel intensities and local geometric constraints, the cerebral WM is first segmented. The WM is divided into 2 hemispheres, and the brain stem and cerebellum are removed. Tessellation is then performed to produce a triangle-based mesh of the WM surface and refined to alleviate the voxel-based nature of the initial curvature. The WM surfaces are deformed outward to generate the pial (GM/CSF intersection) surface. Topologic defects in the surface are corrected by using an automated topology fixer. Visual quality checks are performed and inaccuracies are manually edited and corrected by reprocessing. The cortical surface is spherically inflated so that the entire cortical surface is exposed, including deep tissue inside the sulci. Using combined information from the pial and WM surfaces, cortical thickness is calculated at each vertex.

To perform surface-based analysis of cortical thickness between groups, a custom symmetrical template is constructed by using data from the same 31 control subjects as for VBM and DBM processing. To create a surface template, an average curvature map is created by averaging subject gyral and sulcal curvature patterns. Each study subject's surface is then registered to the template, and the deformation is guided by the cortical features of the template. Thickness data from each subject are then smoothed by using a 20-mm FWHM 2D Gaussian kernel and mapped to an average surface. This average surface is the average of all study subjects for the visualization of results and should not be confused with the template described above.

### **Statistical Analysis**

Linear regression was performed to determine the effect of "group" (patient or control) on the measurement parameter at each voxel/vertex. ICV was entered as a nuisance variable for VBM analysis only

because this was already accounted for during the initial affine registration of DBM and cortical thickness is not confounded by ICV.<sup>29</sup> Contrasts were defined to detect differences at each voxel/vertex between 1) controls and TLE-mts and 2) controls and TLE-no. Given the large number of voxels/vertices being tested in each analysis, it is necessary to correct for multiple comparisons to reduce the probability of obtaining false-positives (type I errors). The most commonly used methods, such as random-field theory and FDR are dependent on the number of voxels/vertices tested. Given that SPM-VBM and DBM images contain approximately 2 million brain voxels, whereas FS provides cortical thickness information at 320,000 vertices on average, these methods of multiple comparison correction make it difficult to fairly compare results across the morphologic methods used in this study. Permutation analysis is a nonparametric technique that has been demonstrated to be an effective multiple comparison correction technique in neuroimaging<sup>30</sup> and is also independent of the number of voxels/vertices tested. A null distribution for the effect of group at each voxel/vertex was constructed by using 10 000 random permutations of the data. For each test, the subject's diagnosis was randomly permuted, and *t* tests were conducted to identify voxels more significant than  $P = .05$ . The group differences more significant than  $P = .05$  were computed for the real experiment and for the random assignments. Finally, a ratio, describing the fraction of the time the suprathreshold group difference was greater in the randomized maps than the real effect (the original labeling), was calculated and a new *P* value was reported for the significance at that point. Voxelwise analysis was conducted by using FSL's "randomize" tool (FMRIB Software Library, version 4; <http://www.fmrib.ox.ac.uk/fsl>). FS-CT analysis was conducted with the same parameters at each vertex by using FS's statistical analysis tool.

## **Results**

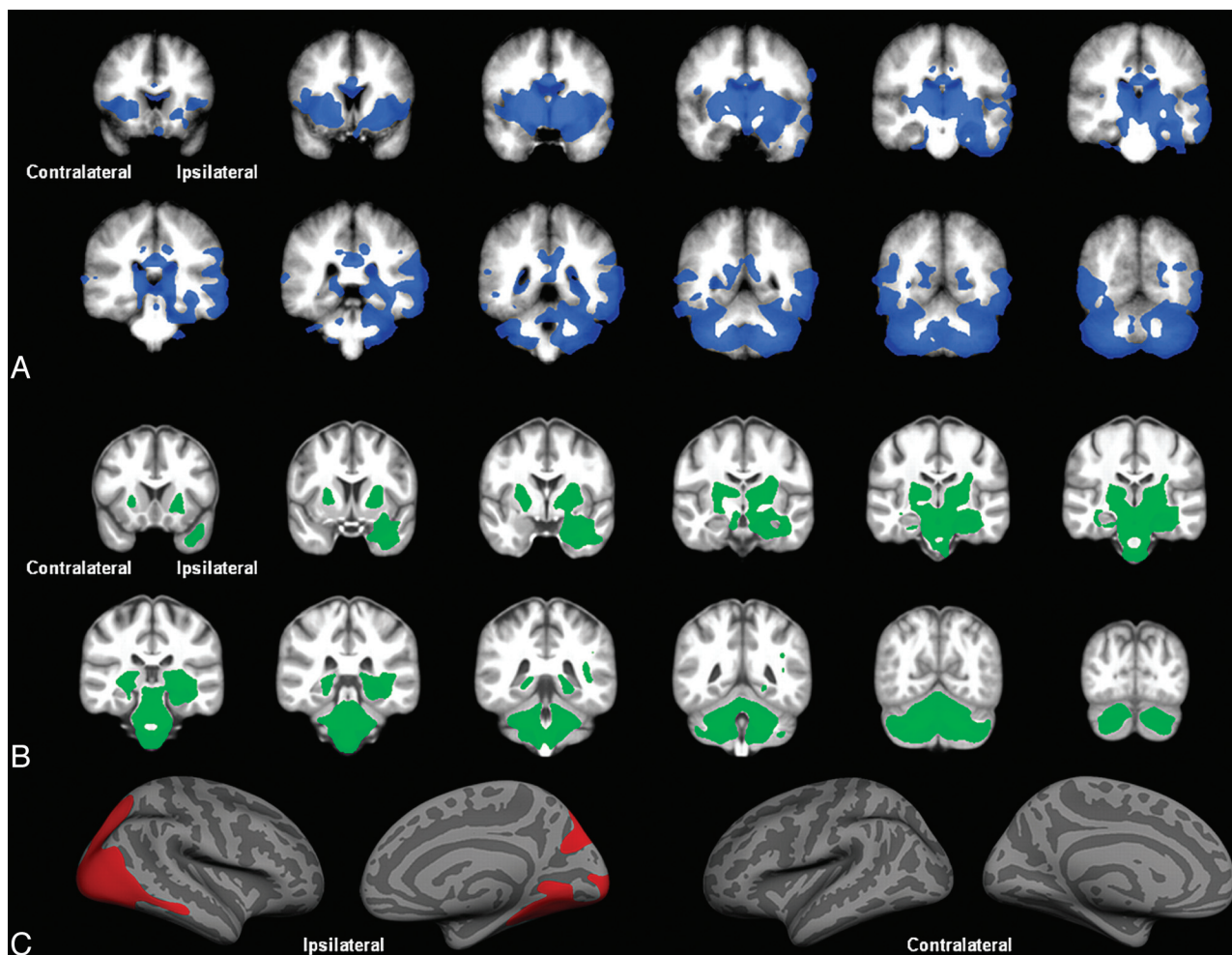
### **TLE-mts versus Controls**

Figure 1 displays GM volume loss (SPM-VBM), volume loss (DBM), and cortical thinning (FS-CT) in TLE-mts compared with controls after permutation correction. Both SPM-VBM and DBM show 1 large cluster of volume losses extending from the ipsilateral hippocampus and mesial temporal lobe to bilateral thalamus, brain stem, and cerebellum. In the SPM-VBM analysis, this cluster extends to the lateral temporo-occipital cortex (ipsilateral > contralateral). FS-CT demonstrates 1 cluster of cortical thinning of the ipsilateral temporo-occipital-parietal region. Table 1 outlines the size of the significant clusters and the maximum *t*-statistic. The largest cluster was found by using VBM analysis; however, DBM revealed the largest cluster *t*-statistic.

### **TLE-no versus Controls**

Figure 2 shows volume loss (DBM) and cortical thinning (FS-CT) in TLE-no compared with controls after permutation correction. SPM-VBM analysis revealed no changes between groups after correction for multiple comparisons. FS-CT showed a large cluster of bilateral cortical thinning in both temporal lobes extending to the frontal, occipital, and parietal lobes bilaterally. DBM demonstrated 2 significant clusters. The first cluster included the ipsilateral temporal lobe, extending to the brain stem and cerebellum. The second cluster included the bilateral superior frontal cortex, pre- and post-central cortex, and superior parietal cortex. Table 2 outlines





**Fig 1.** Controls versus TLE-mts. *A*, VBM-SPM GM differences. *B*, DBM Jacobian differences. *C*, FS-CT differences between groups. All results corrected for multiple comparisons by using permutation analysis ( $P < .05$ ).

Table 1: TLE-mts versus controls			
Method	Region	Cluster Size	Cluster <i>t</i> -Statistic
Freesurfer	Ipsilateral temporo-occipital	20 414.11 mm <sup>2</sup> (70 691 vertices)	6.139
DBM	Bilateral mesial temporal lobe, bilateral thalamus, basal ganglia, subcortical white matter, cerebellum, and brain stem	259 230 mm <sup>2</sup> (259 230 vertices)	7.529
VBM	Ipsilateral mesial temporal lobe, bilateral thalamus, and ipsilateral basal ganglia	282 288 mm <sup>3</sup> (282 288 voxels)	5.693
	Ipsilateral temporal and bilateral occipital cortex		
	Cerebellum and brain stem		

**Note:**—Clusters representing significant differences between controls and TLE-mts for each method after correction for multiple comparisons by using permutation testing.

the size of the significant clusters and the maximum *t*-statistic. Figure 3 shows SPM-VBM, DBM, and FS-CT results after FDR correction for both TLE-mts and TLE-no versus controls.

## Discussion

In this study, we aimed to investigate the aspects of disease atrophy detected by 3 different automated methods of brain morphometry. There were 2 main findings: 1) In TLE-mts, voxel-based methods SPM-VBM and DBM identified the most pronounced volume losses in the ipsilateral hippocampus and mesial temporal region, the ipsi- and contralateral thalamus, and cerebellum. FS-CT showed cortical thinning in the ipsilateral temporo-occipital region. 2) SPM-VBM

showed no significant volume loss in TLE-no. In contrast, DBM detected a region of ipsilateral temporal, bilateral superior frontal, and cerebellar volume loss. The most widespread changes covering the bilateral temporal, frontal, occipital, and parietal cortex were identified by using FS-CT. Based on these findings, we conclude that VBM, DBM, and FS-CT detect different types of atrophy and thus that the choice of the volumetry method should be guided by the knowledge about the disease process.

## TLE-mts

Significant findings after FDR correction were consistent with previous studies, the clinical implications of which

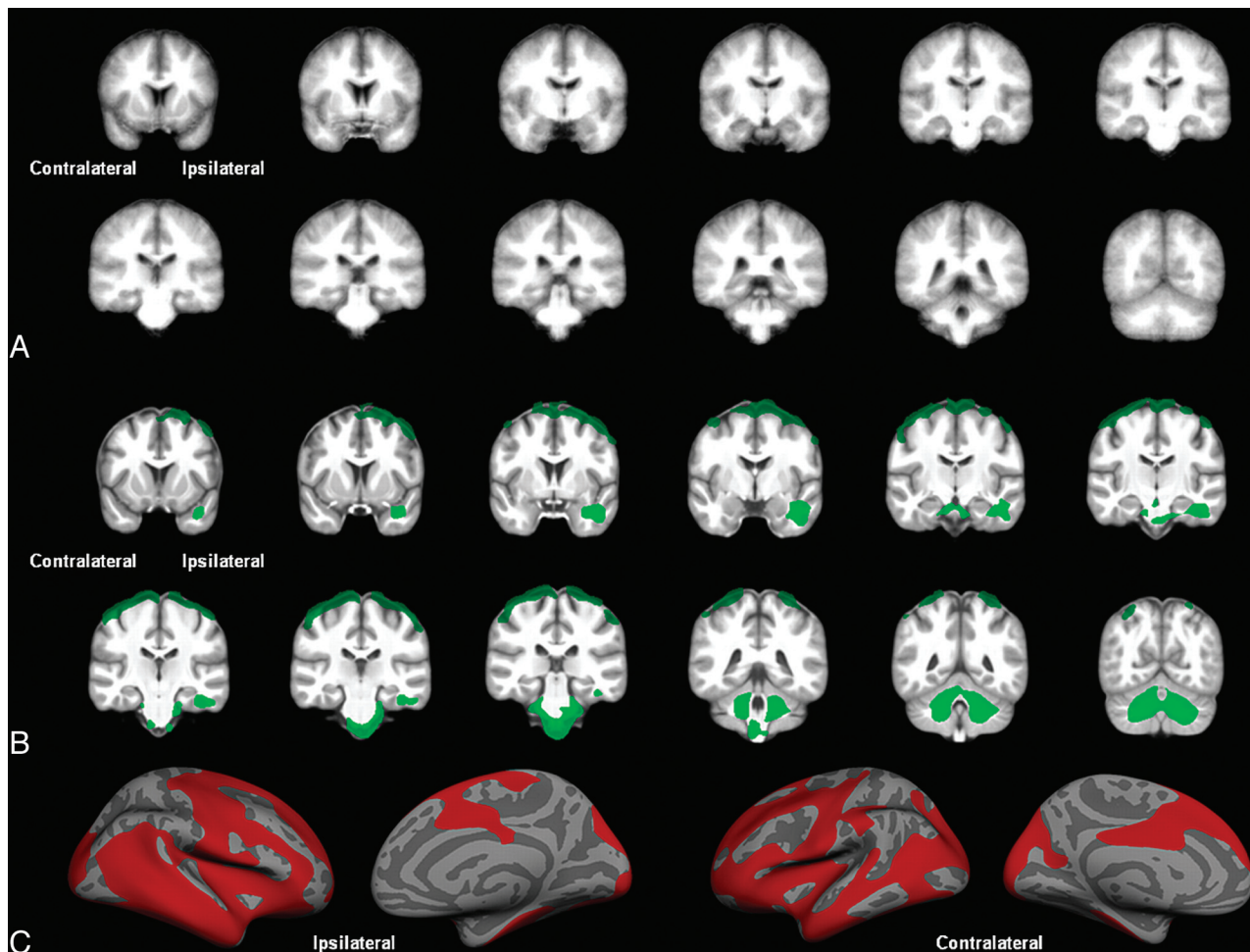


**Fig 2.** Controls versus TLE-no. *A*, VBM-SPM GM differences. *B*, DBM Jacobian differences. *C*, FS-CT differences between groups. All results corrected for multiple comparisons by using permutation analysis ( $P < .05$ ).

**Table 2: TLE-no versus controls**

Method	Region	Cluster Size	Cluster <i>t</i> -Statistic
Freesurfer	Ipsilateral inferior and lateral temporal lobe; insula, posterior, and superior frontal lobe; and lateral and medial occipital region	62 071 mm <sup>2</sup> (70 691 vertices)	7.679
	Contralateral inferior and lateral temporal lobe; insula, posterior, and superior frontal lobe; and lateral and medial occipital region	58 961 mm <sup>2</sup> (66 554 vertices)	4.883
DBM	Cerebellum, brain stem, and ipsilateral temporal lobe	74 453 mm <sup>3</sup> (74 453 voxels)	5.281
	Bilateral superior frontal cortex, pre- and postcentral cortex, and superior parietal cortex	54 397 mm <sup>3</sup> (54 397 voxels)	4.572

**Note:**—Clusters representing significant differences between controls and TLE-no for each method after correction for multiple comparisons by using permutation testing. No significant clusters were found using the VBM method.

have been demonstrated previously and are not discussed here.<sup>9,15,16,18,31,32</sup> The results differ when permutation analysis was used to correct for multiple comparisons instead of the more commonly used FDR approach. These methods of multiple comparison correction are based on different principles (see Statistical Analysis). The permuted results were used to compare between methods because this method is independent of the number of voxels/vertices tested and therefore represents a more unbiased approach.

When comparing across the methodologies, the most

prominent volume changes in TLE-mts were demonstrated below the cortex and identified by using both SPM-VBM and DBM. Both methodologies detected the pathology because the observed changes are macroscopic, and the ability of DBM to detect subtle morphologic changes is not essential. In addition, however, the SPM-VBM cluster extended to the ipsilateral temporal-occipital and contralateral occipital cortex that was not detected by DBM or by previous VBM studies. Although this cortical finding may seem counterintuitive when DBM registration is theoretically

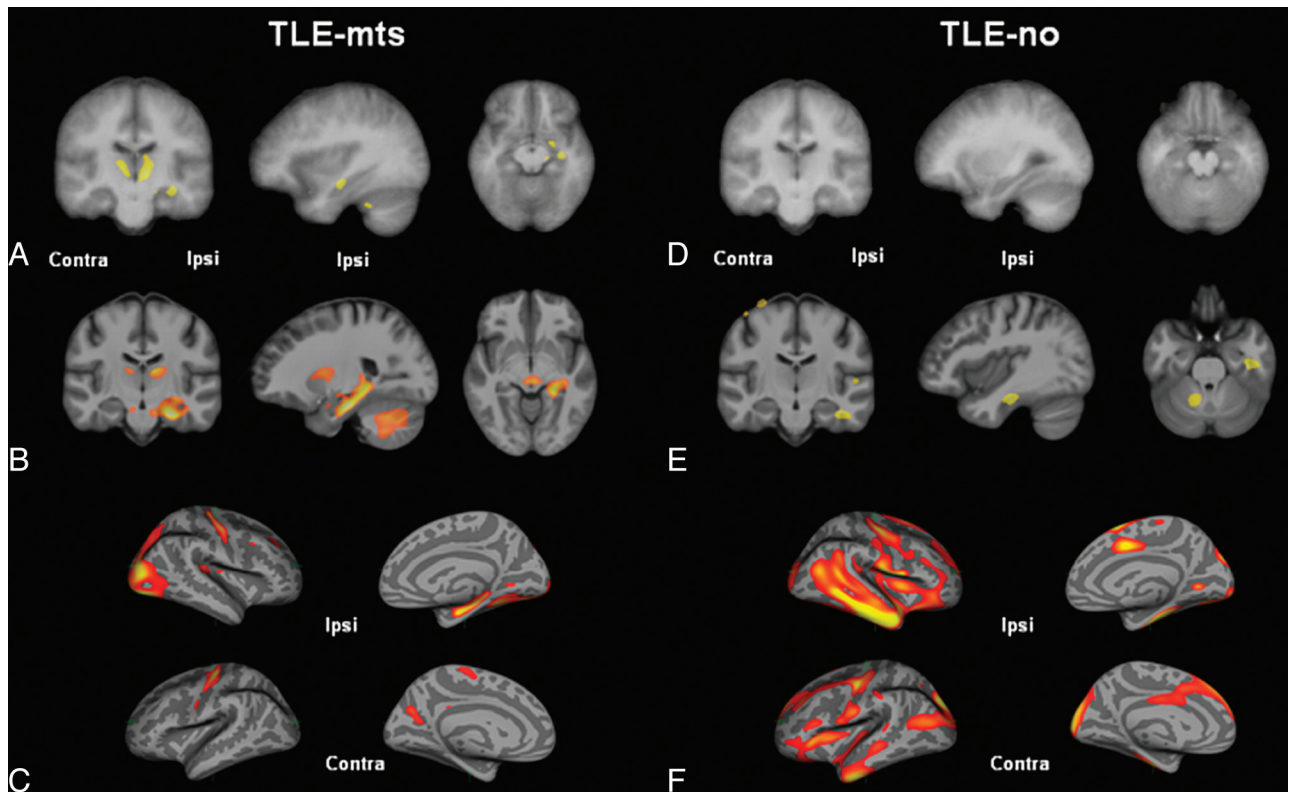


**Fig 3.** Controls versus TLE-mts and controls versus TLE-no after FDR < .05 correction for multiple comparisons. *A*, VBM-SPM GM differences. *B*, DBM Jacobian differences. *C*, FS-CT differences between controls and TLE-mts. *D*, VBM-SPM GM differences. *E*, DBM Jacobian differences. *F*, FS-CT differences between controls and TLE-no.

more accurate than SPM-VBM, there are several possible explanations. 1) An increased intersubject variance in the cortical region by using DBM-SPM-VBM coregistration corrects macroscopic volume effects but maintains most of the individual morphologic differences at the gyral level. DBM, as used in this study, corrects most of the physiologic and disease-related interindividual differences at the gyral level, resulting in a higher between subject variability of the transformation matrix and thus a lower power to detect disease-related differences. 2) Although corrected for head size, the resulting deformation matrix of SPM-VBM contains the affine and the nonlinear transformations, whereas the affine coregistration is not integrated in the DBM transformation matrix. This would suggest that the significant cortical cluster may be a reflection of the volume decrease in the deep WM of the temporal lobe.

FS-CT detected a region of cortical thinning in the temporo-occipital lobe also detected by SPM-VBM. However, volume loss detected by SPM-VBM and DBM mostly affected the hippocampus and subcortical structures that are not part of the FS-CT analysis. These results suggest that TLE-mts is a disease with mostly macroscopic volume loss affecting a large region predominantly including the ipsilateral hippocampus, thalami, and cerebellum, and extending to the lateral temporal cortex, which may be detected best by using VBM analysis. Cortical thinning is present in TLE-mts but, at least in this analysis, is less prominent than the subcortical volume losses that might suggest that the cortical thinning is secondary to the subcortical atrophy.

#### **TLE-no**

The 4T VBM findings presented here were in agreement with previous VBM studies at 1.5T, demonstrating no significant findings after FDR correction.<sup>11,19</sup> The DBM findings were consistent with some previous region of interest volume analyses that show ipsilateral temporal lobe atrophy.<sup>17,18</sup> The FDR corrected cortical thickness results for TLE-no have been reported previously and discussed by our laboratory,<sup>16</sup> but they have not been demonstrated elsewhere.

In the permutation analysis of TLE-no patients versus controls, DBM found significant changes affecting the ipsilateral temporal lobe, cerebellum, and brain stem in 1 cluster, and the superior frontal and parietal cortex in a second cluster. No significant volume loss was detected by using SPM-VBM. This suggests that the fluid-registration algorithm used by DBM may be better suited to detect the subtle volumetric abnormalities associated with this disease type than the spatial basis function algorithm implemented in SPM2. A region of interest-based DBM study focused on the thalamus has previously been carried out on the same study subjects in our laboratory.<sup>33</sup> This study demonstrated a subtle volume loss in this region. If it is necessary to study subcortical structures in disease types with very subtle volume changes such as TLE-no, it may be beneficial to have an a priori hypothesis to avoid having to correct for multiple comparisons across the whole brain, where such a finding may not survive a stringent correction.

FS-CT analysis revealed the most widespread cortical thinning in TLE-no affecting the bilateral temporal lobes, insula,



and frontal and occipital lobes. Only the thinning of the superior frontal cortex also was detected by DBM. The reason for this may be physiologic, methodologic, or a combination: 1) Physiologic: Subtle thinning of the cortex associated with TLE-no is not detected through macroscopic voxel-based volume analysis. The nature of the abnormalities associated with TLE-no may be primarily confined to the thinning of the cerebral cortex, subtle effects of which may be diluted in analysis of volume (a combination of thickness and surface area). In TLE-mts, however, the cortical changes are large and hence can be detected through analysis of either volume or FS-CT. 2) Methodologic: Image registration methods of matching gyral patterns help to precisely colocalize identical cortical regions of subjects without sacrificing the details contained in the underlying measure of interest (ie, FS-CT). Matching intensities, as with SPM-VBM and DBM, is less anatomically meaningful and may lead to a less precise colocalization of subject cortical region and a decrease in the power to detect structural changes in a disease group whose cortical abnormalities are already quite subtle. In addition, the 3D smoothing step used by the voxel-based methods leads to a blurring of tissue across neighboring banks of a sulcus that are not anatomically related and thus could again lead to a reduced ability to detect cortical abnormalities. FS smoothing however is performed across the 2D inflated brain surface, preserving the relationship between neighboring sulcal and gyral structures.

### Limitations

There are several methodologic differences between the techniques that have not been controlled: 1) The methods use different segmentation techniques (probabilistic in SPM-VBM versus binary in FS-CT). 2) Each method requires smoothing for statistical analysis, but because of the different smoothing approaches, it is difficult to determine a comparable smoothing kernel size for surface-based and voxel-based methods. Therefore, in this study, recommendations were taken from previous studies for both voxel- and surface-based smoothing kernel sizes. 3) A more recent SPM toolbox, DARTEL (compatible with SPM, versions 5 and higher) includes an improved atlas creation and registration method that adopts a diffeomorphic registration algorithm that is similar to the DBM approach used in this study.<sup>34</sup> Theoretically, this would lead to more comparable results between VBM-SPM and DBM and is currently being tested in our laboratory. 4) Effort was made to remove brain dura during the skull stripping process before DBM analysis, particularly at the most superior part of the interhemispheric fissure. However, this was difficult to accomplish in some subjects without the removal of cortical voxels. Although the percentage of subjects with some remaining dura between controls and TLE-no subjects was equal, it cannot be disregarded that the superior frontal cortical cluster may be due to this artifact and should be considered a limitation of this method. 5) None of the 3 methods depicts the “whole truth,” ie, just because a brain region seems normal in a VBM or cortical thickness analysis, it cannot be concluded for sure that this structure is not affected by the disease process but only that it is less likely to be affected by the type of pathologic abnormalities to which the chosen method is particularly sensitive.

### Conclusions

The findings of this study show that each of the 3 methods detects different types of structural abnormalities and that the choice of the method has to be guided by the nature of the suspected pathology. Some of the differences are obvious because they are inherent to the method, eg, FS-CT is not suited to detect subcortical abnormalities because these structures are not part of the cortex. However, the results also can differ in structures that are assessed by all 3 methods. Based on the findings in this study, we conclude that SPM-VBM and DBM will detect cortical and subcortical abnormalities in diseases associated by macroscopic volume losses and that FS-CT will detect the cortical component. In diseases without macroscopic volume losses, FS-CT is the optimal method to detect cortical abnormalities. DBM is the optimal method to detect subcortical abnormalities, but DBM also will pick up some of the cortical pathology in these diseases.

Disclosures: Paul Garcia: *Research Support (including provision of equipment or materials):* Medtronic, UCB Pharma *Details:* RCT of thalamic stimulation (Medtronic) and brivaracetam (UCB Pharma). Michael Weiner: *Research Support (including provision of equipment or materials):* NIH, VA, DOD, Merck, Avid *Consultant:* Astra Zeneca, Araclon, Medivation, Pfizer, Ipsen, TauRx, Bayer Healthcare, Biogen Idec, Exonhit Therapeutics, Servier, Synarc.

### References

1. Mechelli A, Price CJ, Friston KJ, et al. **Voxel-based morphometry of the human brain: methods and applications.** *Curr Med Imaging Rev* 2005;1:105–13
2. Wright IC, McGuire PK, Poline JB, et al. **A voxel-based method for the statistical analysis of gray and white matter density applied to schizophrenia.** *Neuroimage* 1995;2:244–52
3. Ashburner J, Hutton C, Frackowiak R, et al. **Identifying global anatomical differences: deformation-based morphometry.** *Neuroimage* 1998;6:348–57
4. Davatzikos C, Vaillant M, Resnick SM, et al. **A computerised approach for morphological analysis of the corpus callosum.** *J Comput Tomogr* 1996;20:88–97
5. Fischl B, Dale AM. **Measuring the thickness of the human cerebral cortex from magnetic resonance images.** *Proc Natl Acad Sci U S A* 2000;97:11050–55
6. Lerch JP, Evans AC. **Cortical thickness analysis examined through power analysis and a population simulation.** *Neuroimage* 2005;24:163–73
7. Bonilha L, Edwards JC, Kinsman SL, et al. **Extrahippocampal gray matter loss and hippocampal deafferentation in patients with temporal lobe epilepsy.** *Epilepsia* 2010;51:519–28
8. Eriksson SH, Thom M, Symms MR, et al. **Cortical neuronal loss and hippocampal sclerosis are not detected by voxel-based morphometry in individual epilepsy surgery patients.** *Hum Brain Mapp* 2009;30:3351–60
9. Keller SS, Roberts N. **Voxel-based morphometry of temporal lobe epilepsy: an introduction and review of the literature.** *Epilepsia* 2008;49:741–57
10. Labate A, Cerasa A, Aguglia U, et al. **Voxel-based morphometry of sporadic epileptic patients with mesiotemporal sclerosis.** *Epilepsia* 2010;51:506–10
11. Riederer F, Lanzenberger R, Kaya M, et al. **Network atrophy in temporal lobe epilepsy: a voxel-based morphometry study.** *Neurology* 2008;71:419–25
12. Good CD, Johnsrude IS, Ashburner J, et al. **A voxel-based morphometric study of ageing in 465 normal adult human brains.** *Neuroimage* 2001a;14:21–36
13. Apostolova LG, Thompson PM. **Brain mapping as a tool to study neurodegeneration.** *Neurotherapeutics* 2007;4:387–400
14. Studholme C, Cardenas V, Blumenfeld R, et al. **Deformation tensor morphometry of semantic dementia with quantitative validation.** *Neuroimage* 2004;21:1387–98
15. Bernhardt BC, Worsley KJ, Besson P, et al. **Mapping limbic network organization in temporal lobe epilepsy using morphometric correlations: insights on the relation between mesiotemporal connectivity and cortical atrophy.** *Neuroimage* 2008;42:515–24
16. Mueller SG, Laxer KD, Barakos J, et al. **Widespread neocortical abnormalities in temporal lobe epilepsy with and without mesial sclerosis.** *Neuroimage* 2009;46:353–59
17. Bernasconi N, Bernasconi A, Caramanos Z, et al. **Entorhinal cortex atrophy in epilepsy patients exhibiting normal hippocampal volumes.** *Neurology* 2001;56:1335–39
18. Mueller SG, Laxer KD, Schuff N, et al. **Voxel-based T2 relaxation rate measurements in temporal lobe epilepsy (TLE) with and without mesial temporal sclerosis.** *Epilepsia* 2007;48:220–28
19. Mueller SG, Laxer KD, Cashdollar N, et al. **Voxel-based optimized morphom-**



- etry (VBM) of gray and white matter in temporal lobe epilepsy (TLE) with and without mesial temporal sclerosis. *Epilepsia* 2006;47:900–07
20. Mueller SG, Laxer KD, Barakos J, et al. Subfield atrophy pattern in temporal lobe epilepsy with and without mesial sclerosis detected by high-resolution MRI at 4 Tesla: preliminary results. *Epilepsia* 2009;50:1474–84
  21. Good CD, Johnsrude IS, Ashburner J, et al. Cerebral asymmetry and the effects of sex and handedness on brain structure: a voxel based morphometric analysis of 465 normal adult human brains. *Neuroimage* 2001b;14:685–700
  22. Van Leemput K, Maes F, Vandermeulen D, et al. Automated model based bias field correction of MR images of the brain. *IEEE Trans Med Imag* 1999;18:885–96
  23. Ashburner J, Friston KJ. Voxel-based morphometry—the methods. *Neuroimage* 2000;11:805–21
  24. Christensen GE, Rabbitt RD, Miller MI. Deformable templates using large deformation kinematics. *IEEE Trans Image Process* 1996;5:1435–47
  25. Lorenzen P, Prastawa M, Davis B, et al. Multi-modal image set registration and atlas formation. *Med Image Anal* 2006;10:440–51
  26. Joshi S, Davis B, Jomier M, et al. Unbiased diffeomorphic atlas construction for computational anatomy. *Neuroimage* 2004;23:151–60
  27. Dale AM, Fischl B, Sereno MI. Cortical surface-based analysis I: segmentation and surface reconstruction. *Neuroimage* 1999;9:179–94
  28. Fischl B, Sereno MI, Dale AM. Cortical surface-based analysis II: inflation, flattening, and a surface-based coordinate system. *Neuroimage* 1999;9:195–207
  29. Barnes J, Ridgway GR, Bartlett J, et al. Head size, age and gender adjustment in MRI studies: a necessary nuisance? *Neuroimage* 2010;53:1244–55
  30. Nichols TE, Holmes AP. Nonparametric permutation tests for functional neuroimaging: a primer with examples. *Hum Brain Mapp* 2001;15:1–25
  31. Lin JJ, Salamon N, Lee AD, et al. Reduced neocortical thickness and complexity mapped in mesial temporal lobe epilepsy with hippocampal sclerosis. *Cereb Cortex* 2007;17:2007–18
  32. McDonald CR, Hagler DJ, Ahmadi ME, et al. Regional neocortical thinning in mesial temporal lobe epilepsy. *Epilepsia* 2008;49:794–803
  33. Mueller SG, Laxer KD, Barakos J, et al. Involvement of the thalamocortical network in TLE with and without mesiotemporal sclerosis. *Epilepsia* 2010;51:1436–45
  34. Ashburner J. A fast diffeomorphic image registration algorithm. *Neuroimage* 2007;38:95–113